Published in final edited form as:
Hum Mol Genet. 2006 September 1; 15(17): 2588–2602.

In vivo function of the orphan nuclear receptor NR2E3 in establishing photoreceptor identity during mammalian retinal development

Hong Cheng[1,2], **Tomas S. Aleman**[4], **Artur V. Cideciyan**[4], **Ritu Khanna**[2], **Samuel G. Jacobson**[4], and **Anand Swaroop**[1,2,3,*]

1 *Neuroscience Graduate Program,*

2 *Department of Ophthalmology and Visual Sciences, W.K. Kellogg Eye Center and*

3 *Department of Human Genetics, University of Michigan, 1000 Wall Street, Ann Arbor, MI 48105, USA and*

4 *Scheie Eye Institute, University of Pennsylvania, Philadelphia, PA, USA*

Abstract

Rod and cone photoreceptors in mammalian retina are generated from common pool(s) of neuroepithelial progenitors. NRL, CRX and NR2E3 are key transcriptional regulators that control photoreceptor differentiation. Mutations in *NR2E3*, a rod-specific orphan nuclear receptor, lead to loss of rods, increased density of S-cones and supernormal S-cone-mediated vision in humans. To better understand its *in vivo* function, *NR2E3* was expressed ectopically in the $Nrl^{-/-}$ retina, where post-mitotic precursors fated to be rods develop into functional S-cones similar to the human *NR2E3* disease. Expression of *NR2E3* in the $Nrl^{-/-}$ retina completely suppressed cone differentiation and resulted in morphologically rod-like photoreceptors, which were however not functional. Gene profiling of FACS-purified photoreceptors confirmed the role of *NR2E3* as a strong suppressor of cone genes but an activator of only a subset of rod genes (including rhodopsin) *in vivo*. Ectopic expression of *NR2E3* in cone precursors and differentiating S-cones of wild-type retina also generated rod-like cells. The dual regulatory function of *NR2E3* was not dependent upon the presence of NRL and/or CRX, but on the timing and level of its expression. Our studies reveal a critical role of *NR2E3* in establishing functional specificity of NRL-expressing photoreceptor precursors during retinal neurogenesis.

INTRODUCTION

Neuronal specification is guided by complex interactions between intrinsic genetic programs and extrinsic regulatory factors, entailing precise coordination between withdrawal from the cell cycle and differentiation (1–5). Acquisition of functional specificity depends on spatially and temporally precise gene expression patterns that are in turn dictated by complex transcriptional regulatory networks (6–8). In the vertebrate retina, six major types of neurons and Müller glia are generated from common pools of multipotent neuroepithelial progenitors in a relatively conserved birth order (7,9). The prevailing model proposes that retinal progenitor cells (RPCs) pass through a series of transient and progressively restricted competence states, in which they can produce a specific set of cell type(s) (9,10). Intrinsic mechanisms appear to

*To whom correspondence should be addressed: Tel: +1 7347633731; Fax: +1 7346470228; Email: swaroop@umich.edu.

Conflict of Interest statement. None declared.

play a major role in retinal cell fate determination (11). Not surprisingly, an array of transcription factors are shown to specify retinal cell fates during development (12–17).

The mammalian retina contains two types of photoreceptors—rods and cones—rods are highly sensitive photoreceptors, whereas cones are responsible for visual acuity, day-light and color vision. In humans and mice, rods greatly outnumber cones and constitute over 95% of photoreceptors. The functional differences between the two photoreceptors are related to their distinct morphology and synaptic connections, and depend upon unique gene expression patterns (18,19). Cones are born earlier than rods during retinal development; however, rod genesis spans a much broader temporal window than cones (20,21). Post-mitotic photoreceptor precursors exhibit variable delays before expressing their respective opsin photopigment (22, 23). The molecular mechanism(s) underlying the 'delay' and gene regulatory networks that dictate photoreceptor maturation have not been precisely elucidated.

Cone-rod homeobox (CRX), neural retina leucine zipper (NRL) and photoreceptor-specific nuclear receptor (NR2E3) are key transcriptional regulators that are shown to control photoreceptor differentiation. The homeodomain protein CRX is required for both rod and cone development and regulates the transcription of many photoreceptor-specific genes (24–26). The Maf-family bZIP transcription factor NRL (27) is essential for rod differentiation and controls the expression of most, if not all, rod specific genes (21,28,29). Its genetic ablation in mouse ($Nrl^{-/-}$) results in the transformation of rod precursors to functional S-cones (15,21, 30). *NR2E3* was first identified by its homology with *Drosophila* developmental gene *tailless* and vertebrate *TLX* (now called *NR2E1*) (31). It appears to be expressed exclusively in the rod photoreceptors (32–35). Mutations in the three regulatory proteins are associated with distinct retinal disease phenotypes (RetNet website: http://www.sph.uth.tmc.edu/RetNet/disease.htm).

Loss-of-function mutations in the human *NR2E3* gene have been identified in patients with enhanced S-cone syndrome (ESCS) and related retinopathies, which are characterized by night-blindness and increased S-cone sensitivity (36–42). A deletion within the mouse *Nr2e3* gene, predicted to result in loss-of-function, is also associated with excess of S-cones and rod degeneration in the *rd7* mouse (43–45). *In vitro* studies have revealed that *NR2E3* activates the promoters of rod-specific genes synergistically with NRL, CRX and other proteins (33, 35) and represses CRX-mediated activation of cone genes (34,35). Aberrant expression of cone-specific genes in the photoreceptor layer of the *rd7* retina further supports the opposing functions of *NR2E3* on rod versus cone genes (34,46). However, *in vivo* function(s) of *NR2E3* in establishing photoreceptor identity and underlying mechanism of enhanced S-cone phenotype produced by *NR2E3* mutations have not been delineated.

In this report, using mouse lines expressing *Nr2e3* transgene in different genetic backgrounds, we demonstrate that ectopic expression of *NR2E3* in photoreceptor precursors completely suppresses cone genes and consequently cone differentiation. Instead, the cones acquire rod-like morphology, but are not photo-responsive because of the lack or low-level expression of several rod phototransduction genes. *NR2E3* has dual function on rod versus cone genes *in vivo*, independent of NRL and/or CRX; nonetheless, it cannot produce functional rods in the absence of NRL. Our studies provide direct evidence in support of NR2E3's role in stabilizing rod developmental pathway during photoreceptor differentiation by suppressing the cone genes in post-mitotic precursors.

RESULTS

Crx promoter directs ectopic expression of *NR2E3* to photoreceptor precursors

To investigate the function of *NR2E3 in vivo*, we took advantage of the $Nrl^{-/-}$ mice (rather than the *rd7* mice), since in the $Nrl^{-/-}$ retina: (1) no endogenous NR2E3 transcript or protein is detectable; (2) rod-specific genes are not expressed; (3) the expression of cone genes is dramatically increased; and (4) the retinal phenotype is easy to distinguish with no rods and only functional cones (15). In addition, we can directly test the function of *NR2E3* without interference from NRL, which can induce rod gene expression (28,29; unpublished data). We generated transgenic mice in the $Nrl^{-/-}$ background using *Crx::Nr2e3* construct (Fig. 1A), in which *Nr2e3* transcription was driven by the *Crx* promoter resulting in its expression in all post-mitotic photoreceptor precursors. The endogenous *Nr2e3* gene and the transgene can be discriminated as 9.0 and 2.8 kb bands, respectively, upon Southern blot analysis of the *Crx::Nr2e3/*$Nrl^{-/-}$ mouse DNA (Fig. 1B). The NR2E3 protein was detected in all six transgenic founders by immunoblot assays (data not shown). The temporal expression of *Nr2e3* transcripts (data not shown) was similar to that of *Crx*, and NR2E3 protein was detected even at embryonic day (E)13 in the transgenic mice (Fig. 1C). By immunohistochemistry (IHC), NR2E3 protein was detected as early as E11 in the dorsal retina (Fig. 1Dc), about 1 week earlier than wild-type (WT) (Fig. 1Dg). At E16, NR2E3 was clearly detectable in the outer neuroblastic layer of the *Crx::Nr2e3/*$Nrl^{-/-}$ transgenic retina but not in WT (Fig. 1Dd–f). At E18, more NR2E3 positive cells were observed in the transgenic mice when compared with WT (Fig. 1Dg and i); however, at P6 and later stages, similar NR2E3 expression levels were detected in both *Crx::Nr2e3/*$Nrl^{-/-}$ and WT retina (Fig. 1C, Dj–l). A 1 h pulse labeling with (+)5-bromo-2′-deoxyuridine (BrdU) did not reveal any BrdU-labeled cells in the E16 retina that also expressed NR2E3 (Fig. 1E). Thus, temporal and spatial expression of NR2E3 in the transgenic mice reflects high fidelity of the 2.3 kb mouse *Crx* promoter.

NR2E3 can repress cone-specific genes and activate rod genes

We examined P21 retinas from all six NR2E3-expressing *Crx::Nr2e3/*$Nrl^{-/-}$ transgenic mouse lines by IHC using antibodies against a number of rod- and cone-specific proteins. In five transgenic lines, rhodopsin was detected in the entire outer nuclear layer (ONL) with slightly stronger signal in the dorsal retina, whereas the $Nrl^{-/-}$ retina showed no rhodopsin staining. Three of the transgenic lines had no S-opsin, M-opsin or cone arrestin labeling (Fig. 2A–C), whereas two others displayed partial expression (data not shown). The sixth transgenic line demonstrated patchy rhodopsin expression in the ONL, with no co-staining of cone-specific markers (data not shown). These data provide a direct support of NR2E3's dual role in regulating rod and cone genes *in vivo*. The three transgenic lines with complete cone gene suppression were used in the following studies.

NR2E3 can partially rescue rod morphology but not function in the $Nrl^{-/-}$ retina

In the WT retina, cones have open outer segment (OS) discs, their cell bodies are located in the outermost rows of the ONL, and their nuclei display punctate staining of the heterochromatin (18). In the $Nrl^{-/-}$ retina, all photoreceptors showed cone-like morphology with whorls and rosettes in the ONL (30). Ectopic expression of NR2E3 in the *Crx::Nr2e3/*$Nrl^{-/-}$ retina resulted in partial transformation from cone- to apparently rod-like photoreceptors in the ONL with no obvious whorls and rosettes; this may be due to elongated OSs and dense nuclear chromatin (Fig. 3A). Notably, oval whorls were still observed on the flat mount retina (data not shown). The ONL was wavy and thinner when compared with the WT retina. Decreased number of cells in the ONL (20–40% less when compared with the WT) was due to increased apoptosis, as indicated by TUNEL staining (data not shown). OS in the *Crx::Nr2e3/*$Nrl^{-/-}$ retina were longer, but still misaligned and shorter than those of the WT (Fig. 3A). The ultrastructure of the OS discs, revealed by transmission electron microscopy

(TEM), showed rod-like closed discs in the *Crx::Nr2e3/Nrl*$^{-/-}$ retina, although the length and orientation of the discs were not as organized as in the WT retina (Fig. 3B). Ectopic expression of NR2E3 can therefore drive photoreceptor precursors towards the rod phenotype, even in the absence of NRL.

We examined retinal function of *Crx::Nr2e3/Nrl*$^{-/-}$ mice by electroretinography (ERG) (Fig. 3C–F). Expectedly, the three transgenic lines with complete suppression of S- and M-opsin showed no detectable ERGs driven by bipolar cells post-synaptic to S- or M-cones. This is in contrast with *Nrl*$^{-/-}$ mice where post-receptoral S-cone responses were nearly 10-fold greater in amplitude when compared with WT (Fig. 3C and D). Unexpectedly, even though there was high expression of rhodopsin (Fig. 2), all animals from these transgenic lines showed no detectable ERGs when presented with stimuli known to activate rod photoreceptors (Fig. 3E and F, and data not shown). Under these dark-adapted conditions, activity of rod bipolar cells dominate ERG b-waves from −4 to −1 log scot-cd.s.m^{-2} in WT mice; cone-derived function contributes increasingly at higher intensities as seen from the cone-only responses of *Nrl*$^{-/-}$ mouse (Fig. 3E and F) (15,30). ERG photoresponses directly originating from photoreceptor activity were also extinguished (Fig. 3E and F, and data not shown). With the paired high-intensity photoresponses used, rod activity normally dominates the first flash response (Fig. 3F, black traces); and, cone activity dominates the second flash response. In the *Nrl*$^{-/-}$ mice, photoresponses were smaller (68 ± 18 versus 377 ± 133 μV) and slower (1.93 ± 0.35 versus 3.33 ± 0.13 log scot-cd^{-1}.m^{2}.s^{-3}) than those driven by WT rods, but they were larger than those driven by WT cones (Fig. 3F).

The two *Crx::Nr2e3/Nrl*$^{-/-}$ lines with incomplete cone suppression showed recordable ERGs with abnormal b-wave amplitudes and threshold elevations similar to the *Nrl*$^{-/-}$ mice but with smaller amplitudes. In these lines, there was also no evidence of rod function, but there was detectable cone function, which was enriched in S-cone activity (data not shown). ERG responses to the short wavelength stimulus in these lines were three to four times larger than those evoked by the longer wavelength flash; this ratio was three to six times in the *Nrl*$^{-/-}$ mice. The transgenic line with minor cone-opsin suppression revealed ERGs similar to those of the *Nrl*$^{-/-}$ mice (data not shown).

Lack of rod function in the *Crx::Nr2e3/Nrl*$^{-/-}$ retina is associated with reduced or no expression of several rod phototransduction genes

To investigate the underlying cause of the apparent lack of rod activity, despite the existence of rod-like cells with high rhodopsin expression, we performed quantitative RT–PCR (qPCR) analysis of phototransduction genes using total RNA from the WT, *Nrl*$^{-/-}$ and *Crx::Nr2e3/Nrl*$^{-/-}$ retina. We observed dramatically lower expression of genes encoding cone phototransduction proteins (such as *S-opsin*, *M-opsin*, *Gnat2*, *Pde6c* and *Arr3*) in the *Crx::Nr2e3/Nrl*$^{-/-}$ retina when compared with *Nrl*$^{-/-}$; however, among the rod genes tested by qPCR only *rhodopsin* transcripts were dramatically increased and almost reached the level of the WT (Fig. 4). While a few of the rod phototransduction genes, such as *Pde6b* and *Cnga1*, exhibited higher yet variable level of expression, the transcripts for alpha subunit of rod transducin, *Gnat1*, were undetectable as in the *Nrl*$^{-/-}$ mouse (Fig. 4). It therefore appears that NR2E3 cannot direct the expression of the full complement of rod-specific genes when NRL is not present. Consistent with our findings, *Gnat1* knockout mice have no rod ERG but do show relatively normal retinal morphology (47).

Potential downstream targets of NR2E3 identified by gene profiling of FACS-purified photoreceptors

To validate qPCR results and explore additional possible downstream targets of NR2E3, we mated the transgenic mice with the *Nrl::GFP* transgenic mice, in which the expression of GFP

is driven by an *Nrl* promoter (21). In the resulting *Nrl::GFP/Crx::Nr2e3/Nrl*$^{-/-}$ mice, all rod photoreceptors are specifically tagged with GFP and can therefore be purified by fluorescence-activated cell sorting (FACS). We performed expression profiling of FACS-purified GFP+ cells from *Nrl::GFP/Crx::Nr2e3/Nrl*$^{-/-}$ mice at 4 weeks. The comparison of gene profiles to those of GFP+ cells from *Nrl::GFP*/*Nrl*$^{-/-}$ and *Nrl::GFP*/WT mice (21) revealed that ectopic expression of NR2E3 suppressed a large number of genes, which were up-regulated in the *Nrl::GFP*/*Nrl*$^{-/-}$ retina (Table 1). Several of these genes are known to be preferentially expressed in cone photoreceptors (Fig. 4). Interestingly, a much smaller set of genes was upregulated upon expression of NR2E3 in the *Nrl*$^{-/-}$ retina; whereas rhodopsin was among the genes induced by NR2E3, several rod phototransduction genes showed only marginal or no increase in expression when compared with the *Nrl*$^{-/-}$ retina (Table 1; data not shown). These differentially expressed genes in the *Crx::Nr2e3/Nrl*$^{-/-}$ retina, compared with *Nrl*$^{-/-}$ retina, are potentially direct downstream targets of NR2E3.

CRX is not necessary for NR2E3-mediated gene regulation

To evaluate the hypothesis that CRX is required for NR2E3-mediated transcriptional regulation (35), we mated *Crx::Nr2e3/Nrl*$^{-/-}$ mice with the *Nrl* and *Crx* double knockout (*Nrl*$^{-/-}$/*Crx*$^{-/-}$) mice. In the *Nrl*$^{-/-}$/*Crx*$^{-/-}$ retina, M-opsin is barely detectable (data not shown) because of the *Crx*$^{-/-}$ background (48); however, S-opsin and cone arrestin are enriched and rhodopsin is undetectable because of the absence of NRL (Fig. 5; data not shown). In the *Crx::Nr2e3/Nrl*$^{-/-}$/*Crx*$^{-/-}$ retina, ectopic expression of NR2E3 results in complete suppression of S-opsin and cone arrestin, whereas rhodopsin staining is observed in the ONL (Fig. 5; data not shown). A few rhodopsin positive cells are found even in the inner nuclear layer (INL) of the *Crx::Nr2e3/Nrl*$^{-/-}$/*Crx*$^{-/-}$ retina (data not shown), probably reflecting migration defects. These data suggest that NR2E3 can directly modulate rod and cone specification even in the absence of CRX and/or NRL.

NR2E3 transforms cone precursors to rod-like cells in the WT retina

To further examine NR2E3 function, we transferred the *Crx::Nr2e3* transgene to the WT background. Expression of rhodopsin in the *Crx::Nr2e3*/WT retina was similar to WT; however, no cone-specific markers were detected (Fig. 6A). The retinal histology was apparently normal in the transgenic mice, except that cone-like nuclei were not observed (Fig. 6B). To determine the fate of cone precursors in the *Crx::Nr2e3*/WT retina, we injected a single dose of BrdU in the pregnant mice at day 14 after fertilization (note that E13–E14 represents the peak of cone genesis) and analyzed the retinas at P21. The number of strongly BrdU-labeled cells in the ONL near the optic nerve was not altered in transgenic retinas when compared with WT retinas (data not shown); however, there was a difference in the location of these cells. In the WT retina, strongly BrdU-labeled cells were observed in both the inner and outer halves of the ONL, and most cells in the outer half co-expressed cone markers, such as S-opsin (Fig. 6Ca–d). In the transgenic retina, almost all strongly BrdU-labeled cells were located in the inner part of the ONL (Fig. 6Ce–f). TUNEL staining at E16, P2, P6, P10 and 4 weeks did not reveal any obvious differences between the WT and transgenic retinas (data not shown). We propose that NR2E3 expression forces the early-born cone precursors to adopt the rod-like phenotype; these cells stay in the inner part of the ONL with other early-born rods and do not migrate to the outer part of the ONL as WT cones.

ERGs from the *Crx::Nr2e3*/WT transgenic mice show normal rod responses but undetectable S- or M-cone responses (Fig. 6D). Thus, these retinas contain only rod photoreceptors.

Ectopic expression of NR2E3 transforms differentiating S-cones into rod-like cells

We then wanted to test whether ectopic expression of NR2E3 can also suppress phototransduction genes in differentiating cones. We therefore expressed NR2E3 under the

control of *S-opsin* promoter (49) in both $Nrl^{-/-}$ and WT genetic backgrounds (Fig. 7). In the *S-opsin::Nr2e3/*$Nrl^{-/-}$ retina, the temporal expression of *Nr2e3* transcripts was similar to S-opsin in the early developmental stages but decreased after 3 weeks, and the protein amounts appeared considerably lower than the WT (Fig. 7C and D). Rhodopsin was detected in the ONL and OSs (Fig. 7G–J) and was predominantly distributed in the dorsal retina (data not shown). In retinal sections and whole mounts, rhodopsin and cone proteins did not colocalize (Fig. 7G and J). A few of the nuclei in the ONL of the *S-opsin::Nr2e3/*$Nrl^{-/-}$ retina showed rod-like morphology and the OSs were rod-like (closed discs and long) but were distorted when compared with the $Nrl^{-/2}$ retina (Fig. 7E and F). ERG studies showed no differences in visual function between the transgenic and the $Nrl^{-/-}$ mice (data not shown). qPCR analysis revealed the absence of *Gnat1* transcripts in the *S-opsin::Nr2e3/*$Nrl^{-/-}$ retina although rhodopsin expression could be detected (data not shown). A less dramatic phenotype in the *S-opsin::Nr2e3* retina when compared with the *Crx::Nr2e3* mice is probably because of the expression time and levels of NR2E3 in developing cones. The reduced level of NR2E3 in *S-opsin::Nr2e3* retina may reflect an equilibrium between the NR2E3 expression driven by the *S-opsin* promoter and its subsequent repression by NR2E3 itself.

In the *S-opsin::Nr2e3/*WT mice, retinal morphology and ERGs showed no obvious difference from WT (data not shown). Although the dorsal–ventral pattern of S-opsin gradient was not altered in the *S-opsin::Nr2e3/*WT retina, the number of S-opsin positive cells was decreased in retinal flat mounts (Fig. 7K and L) and sections (data not shown). Cone arrestin positive cells were also reduced but not the M-opsin positive cells (data not shown).

DISCUSSION

Nuclear receptors (NRs) are ligand-dependent transcription factors that regulate critical biological processes and integrate responses to diverse signaling pathways (50,51). The function of NRs can switch, depending on the context, from gene activation to repression, and be modulated by preferential recruitment of regulatory cofactors in response to molecular cues (such as binding of a ligand or post-translational modifications) (52). Here, we demonstrate that NR2E3 has a critical role in photoreceptor development. We show that the primary role of NR2E3 in post-mitotic photoreceptor precursors is to suppress the expression of cone genes, thereby facilitating the induction of rod differentiation. On its own, NR2E3 cannot directly produce the functional rods; nonetheless, it does activate some of the rod-specific genes and leads to rod-like morphology. The dual function of NR2E3 in gene regulation does not require NRL or CRX as revealed by studies in $Nrl^{-/-}$ and $Crx^{-/-}$ backgrounds; however, as suggested (33), the endogenous function of NR2E3 is likely to be accomplished synergistically with CRX and NRL during normal rod development. *In vitro* studies showing repression of CRX-mediated transactivation of cone opsin promoters by NR2E3 (34,35) support our *in vivo* findings of the dual and opposing functions of NR2E3 on rod versus cone gene expression. We propose that NR2E3 function is essential to stabilize the rod cell lineage in photoreceptor precursors, allowing their subsequent differentiation into functional rods.

The expression of NR2E3 in new-born and developing rods (32,33) suggests that it functions in integrating gene regulatory networks, which guide the differentiation of post-mitotic precursors to functional rod photoreceptors. The timing and level of NR2E3 expression appear to be critical since the *S-opsin::Nr2e3* transgene, which is activated later in development, induces rod morphology and rod-specific genes to a much lesser extent when compared with NR2E3 driven by the *Crx* promoter, which is activated earlier in photoreceptor precursors. When expressed early in post-mitotic precursors under control of *Crx* promoter, NR2E3 is able to completely suppress cone photoreceptor function (as measured by ERG response) in the WT and $Nrl^{-/-}$ retina. However, although the presumptive cones acquire rod-like morphology in the $Nrl^{-/-}$ background they do not exhibit rod function. This is probably because, in the absence

of NRL, NR2E3 fails to activate expression of many rod genes, including rod transducin, Gnat1 which is an essential G-protein in the rod phototransduction pathway. A putative NR2E3-binding site could not be identified within the 2 kb promoter region of *Gnat1* though a half site of the consensus core sequence was present in the *Pde6b* promoter. Earlier *in vitro* studies showed that NR2E3 could activate *Gnat1* and *Pde6b* promoters, but only synergistically with NRL and CRX (33). The low or no expression of many rod-specific genes may account for early onset degeneration of some of the rod-like photoreceptors in the transgenic mice, resulting in a thinner ONL.

The gene profiling of the purified GFP+ cells from the WT, *Nrl*$^{-/-}$ and *Crx::Nr2e3/Nrl*$^{-/-}$ retina reveals that NRL and NR2E3 serve critical yet distinct roles in mammalian photoreceptor development. While NRL is a strong activator of rod-specific gene expression, NR2E3 seems to primarily act as a transcriptional repressor of cone genes, and this function does not require NRL. We propose that NR2E3 is also a transcriptional co-activator of rod genes in the presence of NRL, as indicated by *in vitro* data (33). Investigations of retinopathy patients with *NR2E3* mutations suggest developmental defects in both rod and cone photoreceptors (36–39,44). We suggest that aberrant or loss of NR2E3 function causes de-repression of cone genes in the developing rod photoreceptors with predominantly S-cone characteristics. Notably, S-opsin is the first visual pigment to appear in the human fetal retina and S-cones account for over 90% of the retina at fetal week 19, with subsequent decrease as development proceeds (23). It is therefore possible that many of these S-cones acquire rod phenotype upon NRL and NR2E3 expression. The loss of NR2E3 in patients may not permit suppression of S-cone genes leading to ESCS.

Our microarray analysis of the GFP+ cells also revealed that NR2E3 altered the expression of many non-photoreceptor-specific genes; these include apoptotic markers (e.g. Caspase 7), transport proteins (such as potassium channels Kcne2 and Kcnj14) and transcription factors (like Eya1). This might reflect a stress-induced behavior of non-functional and partly developed rod-like photoreceptors in *Crx::Nr2e3/Nrl*$^{-/-}$ retina. It is also likely that some of the expression changes demonstrate a wider role of NR2E3 regulatory network, involving trophic effects, down-regulation of apoptosis, switching of metabolic functions etc. Further investigations are necessary to elucidate additional functions of NR2E3.

In summary, we have demonstrated bimodal functionality of the orphan nuclear receptor NR2E3 *in vivo* during photoreceptor development. Based on previous studies (15,44) and the data reported here, we propose that at least two independent pathways downstream of NRL must function concurrently and synergistically to produce fully functional rods. One of these pathways requires NR2E3, which works with other co-regulators to repress cone genes. In the second pathway, NR2E3 acts as a co-activator of NRL and CRX to achieve quantitatively precise expression of many (if not all) rod-specific genes. Fine-tuning of gene expression patterns requires combinatorial action of distinct transcriptional regulators (53). We suggest that NR2E3 expression is necessary to suppress cone genes in NRL-expressing photoreceptor precursors, and this in turn stabilizes the transcriptional program to generate functional rods (Fig. 8). Notably, the quantitatively precise spatiotemporal coordination of gene expression that nuclear receptors orchestrate in response to molecular cues is mediated, to a large extent, by ligand-binding and protein–protein interactions (50,52,54). Therefore, the identification of natural ligand(s) (if any) of NR2E3 and/or its co-regulators would be valuable for developing novel approaches to treat specific retinal degenerative diseases by modulating gene expression in photoreceptors.

MATERIALS AND METHODS

Transgenic mice

A 2.3 kb mouse *Crx* promoter DNA (from −2286 to +72, GenBank accession nos AF335248 and AF301006; (55) and the *Nr2e3*-coding region (GenBank accession no. NM013708) with an additional Kozak sequence (indicated as underlined letters) was amplified as a *BglII–NotI* (restriction enzyme sites are indicated as bold letters) fragment by PCR (forward primer: GAC**AGATCT***GCCACC*ATGAGCTCTACAGTGGCT; reverse primer: CACTTGGC**GCGGCCGC**CTAGTTTTTGAACATGT) from mouse retina cDNA and cloned into *BamHI–NotI* sites of pcDNA4/HisMaxC (Invitrogen). Then the *KpnI–NotI* fragment was cloned into a modified promoter-less pCl (pCIpl) vector (49) as shown (Fig. 1A). The 4.2 kb *Crx::Nr2e3* fragment was purified and injected into fertilized $Nrl^{-/-}$ (mix background of 129X1/SvJ and C57BL/6J) mouse oocytes (UM transgenic core facility). Transgenic founder mice and their progeny were identified by PCR, and then confirmed by Southern blot analysis of tail DNA. Transgenic founders were bred to the $Nrl^{-/-}$ mice to generate F1 progeny. The transgenic progeny was also mated to C57BL/6J or $Nrl^{-/-}/Crx^{-/-}$ mice to generate *Crx::Nr2e3*/WT or *Crx::Nr2e3*/$Nrl^{-/-}/Crx^{-/-}$ mice, respectively. The *S-opsin:: Nr2e3* transgenic mice were generated in a similar manner, except that a 520 bp mouse *S-opin* promoter DNA (from −870 to −346, Genbank accession no. L27831) (49) was used.

All studies involving mice were performed in accordance with institutional and federal guidelines and approved by the University Committee on Use and Care of Animals at the University of Michigan.

DNA, RNA and protein analysis

Standard protocols were used for Southern analysis, PCR, qPCR, immunoblotting and immunofluorescence experiments (15,21). The primary antibodies used in this study were: rabbit anti-NR2E3 antibody (33), rabbit anti S-opsin, M-opsin or mouse cone arrestin polyclonal antibodies (generous gifts from C. Craft), mouse anti-rhodopsin (4D2) monoclonal antibody (generous gift from R. Molday), mouse anti-γ tubulin monoclonal antibody (Sigma) and rat anti-BrdU monoclonal antibody (BU1/75, Harlan Sera-Lab, Loughborough, UK). Fluorescent detection was performed using AlexaFluor-488, 546 or 633 (Molecular Probes) and Texas Red (Jackson ImmunoResearch, West Grove, PA, USA) conjugated secondary antibodies. Sections were visualized under a conventional fluorescent microscope or FV500 Confocal microscope and digitized.

BrdU labeling

Timed-pregnant females or pups received a single intraperitoneal injection of BrdU (BrdU, Sigma; 0.1 mg/g body weight). The eyes were fixed in 4% paraformaldehyde and cryosectioned at 3 weeks of age. IHC and BrdU staining were performed as described (21).

Transmission electron microscopy

Mice were perfusion-fixed with 2.5% glutaraldehyde in 0.1 M Sorensen's buffer, pH 7.4. Eye cups were excised, fixed, dehydrated and then embedded in Epon epoxy resin following the standard protocol. Semi-thin sections were stained with toluidine blue for tissue orientation. Central part of the dorsal retina was ultra-thin sectioned (70 nm in thickness) and stained with uranyl acetate and lead citrate. The sections were examined using a Philips CM100 electron microscope at 60 kV. Images were recorded digitally using a Hamatsu ORCA-HR digital camera system operated using AMT software (Advanced Microscopy Techniques Corp., Danvers, MA, USA).

FACS enrichment and microarray analysis

Methods for microarray analysis have been described previously (21,29,56). Mouse retinas were dissected at 4 week. GFP+ photoreceptors were enriched by FACS (FACSAria, BD Biosciences, Franklin Lakes, NJ, USA). RNA was extracted from $1 \sim 5 \times 10^5$ flow-sorted cells using Trizol (Invitrogen). Total RNA (40–60 ng) was used for linear amplification with Ovation Biotin labeling system (Nugen), and 2.75 μg of biotin-labeled fragmented cDNA was hybridized to mouse GeneChips MOE430.2.0 (Affymetrix) having 45 101 probesets (corresponding to over 39 000 transcripts and 34 000 annotated mouse genes). Four independent samples were used for each time point. Normalized data were subjected to two-stage analysis based on false discovery rate with confidence interval (FDRCI) for screening differentially expressed genes (24,27) with a minimum fold change of 4.

Electroretinograms

Dark-adapted (>6 h) ERGs in response to increasing intensities (−4.2 to 0.3 log scot-cd.s.m^{-2}) of blue lights were recorded from anesthetized mice using a computer-based system as described (57). The threshold intensity that evokes a criterion (20 μV) dark-adapted b-wave was determined by plotting its amplitude as a function of stimulus intensity and linearly interpolating the stimulus intensity value that corresponded to the criterion. Dark-adapted photoresponses were then elicited with a pair of flashes (white; 3.6 log scot-cd.s.m^{-2}) presented 4 s apart and were fit with a model of phototransduction activation (58). A second computer-based system (Espion, Diagnosys LLC, Littleton, MA, USA) was used to generate light-adapted (40 cd.m^2 white background) ERGs in response to a Xenon UV flash (360 nm peak, Hoya U-360 filter, Edmund Optics, Barrington, NJ, USA). The energy of this flash was adjusted to evoke responses matched in waveform to those elicited with green LEDs (510 nm peak; 0.87 log phot-cd.s.m^{-2}, 4 ms) stimulus in WT mice. These stimuli were presented in a Ganzfeld lined with aluminum foil (59).

Acknowledgements

We thank P. Raymond, P.F. Hitchcock, T. Glaser, D. Goldman, R. Koenig, M. Uhler, A.J. Mears, E. Oh, T. Saunders, J.S. Friedman and H. Khanna for stimulating discussions and/or comments on the manuscript. The *Crx*$^{-/-}$ mice were kindly provided by C. Cepko (Harvard). We acknowledge S. Lenz for confocal facility (of Michigan Diabetes Research and Training Center), M. Gillett, D. Molnar, B. Popoola, S. Reske, M. Van Keuren and D. Wilson for technical assistance, A. Roman for help with electrophysiology recordings, and S. Ferrara for administrative support. This research was supported by grants from the National Institutes of Health (EY011115, EY014259, EY007003, EY013934, DK020572), The Foundation Fighting Blindness, Macula Vision Research Foundation, Research to Prevent Blindness and Elmer and Sylvia Sramek Foundation.

References

1. Ericson J, Morton S, Kawakami A, Roelink H, Jessell TM. Two critical periods of Sonic Hedgehog signaling required for the specification of motor neuron identity. Cell 1996;87:661–673. [PubMed: 8929535]
2. Desai AR, McConnell SK. Progressive restriction in fate potential by neural progenitors during cerebral cortical development. Development 2000;127:2863–2872. [PubMed: 10851131]
3. Levine EM, Fuhrmann S, Reh TA. Soluble factors and the development of rod photoreceptors. Cell Mol Life Sci 2000;57:224–234. [PubMed: 10766019]
4. Dyer MA, Cepko CL. Regulating proliferation during retinal development. Nat Rev Neurosci 2001;2:333–342. [PubMed: 11331917]
5. Ohnuma S, Harris WA. Neurogenesis and the cell cycle. Neuron 2003;40:199–208. [PubMed: 14556704]
6. Brivanlou AH, Darnell JE Jr. Signal transduction and the control of gene expression. Science 2002;295:813–818. [PubMed: 11823631]
7. Marquardt T, Gruss P. Generating neuronal diversity in the retina: one for nearly all. Trends Neurosci 2002;25:32–38. [PubMed: 11801336]

8. Levine M, Davidson EH. Gene regulatory networks for development. Proc Natl Acad Sci USA 2005;102:4936–4942. [PubMed: 15788537]
9. Livesey FJ, Cepko CL. Vertebrate neural cell-fate determination: lessons from the retina. Nat Rev Neurosci 2001;2:109–118. [PubMed: 11252990]
10. Cepko CL, Austin CP, Yang X, Alexiades M, Ezzeddine D. Cell fate determination in the vertebrate retina. Proc Natl Acad Sci USA 1996;93:589–595. [PubMed: 8570600]
11. Cayouette M, Barres BA, Raff M. Importance of intrinsic mechanisms in cell fate decisions in the developing rat retina. Neuron 2003;40:897–904. [PubMed: 14659089]
12. Burmeister M, Novak J, Liang MY, Basu S, Ploder L, Hawes NL, Vidgen D, Hoover F, Goldman D, Kalnins VI, et al. Ocular retardation mouse caused by Chx10 homeobox null allele: impaired retinal progenitor proliferation and bipolar cell differentiation. Nat Genet 1996;12:376–384. [PubMed: 8630490]
13. Mathers PH, Grinberg A, Mahon KA, Jamrich M. The Rx homeobox gene is essential for vertebrate eye development. Nature 1997;387:603–607. [PubMed: 9177348]
14. Marquardt T, Ashery-Padan R, Andrejewski N, Scardigli R, Guillemot F, Gruss P. Pax6 is required for the multipotent state of retinal progenitor cells. Cell 2001;105:43–55. [PubMed: 11301001]
15. Mears AJ, Kondo M, Swain PK, Takada Y, Bush RA, Saunders TL, Sieving PA, Swaroop A. Nrl is required for rod photoreceptor development. Nat Genet 2001;29:447–452. [PubMed: 11694879]
16. Nishida A, Furukawa A, Koike C, Tano Y, Aizawa S, Matsuo I, Furukawa T. Otx2 homeobox gene controls retinal photoreceptor cell fate and pineal gland development. Nat Neurosci 2003;6:1255–1263. [PubMed: 14625556]
17. Hatakeyama J, Kageyama R. Retinal cell fate determination and bHLH factors. Semin Cell Dev Biol 2004;15:83–89. [PubMed: 15036211]
18. Carter-Dawson LD, LaVail MM. Rods and cones in the mouse retina. I Structural analysis using light and electron microscopy. J Comp Neurol 1979;188:245–262. [PubMed: 500858]
19. Jacobs GH. The distribution and nature of colour vision among the mammals. Biol Rev Camb Phil Soc 1993;68:413–471.
20. Carter-Dawson LD, LaVail MM. Rods and cones in the mouse retina. II Autoradiographic analysis of cell generation using tritiated thymidine. J Comp Neurol 1979;188:263–272. [PubMed: 500859]
21. Akimoto M, Cheng H, Zhu D, Brzezinski JA, Khanna R, Filippova E, Oh EC, Jing Y, Linares JL, Brooks M, et al. Targeting of GFP to newborn rods by Nrl promoter and temporal expression profiling of flow-sorted photoreceptors. Proc Natl Acad Sci USA 2006;103:3890–3895. [PubMed: 16505381]
22. Morrow EM, Belliveau MJ, Cepko CL. Two phases of rod photoreceptor differentiation during rat retinal development. J Neurosci 1998;18:3738–3748. [PubMed: 9570804]
23. Xiao M, Hendrickson A. Spatial and temporal expression of short, long/medium, or both opsins in human fetal cones. J Comp Neurol 2000;425:545–559. [PubMed: 10975879]
24. Chen S, Wang QL, Nie Z, Sun H, Lennon G, Copeland NG, Gilbert DJ, Jenkins NA, Zack DJ. Crx, a novel Otx-like paired-homeodomain protein, binds to and transactivates photoreceptor cell-specific genes. Neuron 1997;19:1017–1030. [PubMed: 9390516]
25. Furukawa T, Morrow EM, Cepko CL. Crx, a novel otx-like homeobox gene, shows photoreceptor-specific expression and regulates photoreceptor differentiation. Cell 1997;91:531–541. [PubMed: 9390562]
26. Freund CL, Gregory-Evans CY, Furukawa T, Papaioannou M, Looser J, Ploder L, Bellingham J, Ng D, Herbrick JA, Duncan A, et al. Cone-rod dystrophy due to mutations in a novel photoreceptor-specific homeobox gene (CRX) essential for maintenance of the photoreceptor. Cell 1997;91:543–553. [PubMed: 9390563]
27. Swaroop A, Xu JZ, Pawar H, Jackson A, Skolnick C, Agarwal N. A conserved retina-specific gene encodes a basic motif/leucine zipper domain. Proc Natl Acad Sci USA 1992;89:266–270. [PubMed: 1729696]
28. Rehemtulla A, Warwar R, Kumar R, Ji X, Zack DJ, Swaroop A. The basic motif-leucine zipper transcription factor Nrl can positively regulate rhodopsin gene expression. Proc Natl Acad Sci USA 1996;93:191–195. [PubMed: 8552602]
29. Yoshida S, Mears AJ, Friedman JS, Carter T, He S, Oh E, Jing Y, Farjo R, Fleury G, Barlow C, Hero AO, Swaroop A. Expression profiling of the developing and mature *Nrl*$^{-/-}$ mouse retina:

identification of retinal disease candidates and transcriptional regulatory targets of Nrl. Hum Mol Genet 2004;13:1487–1503. [PubMed: 15163632]

30. Daniele LL, Lillo C, Lyubarsky AL, Nikonov SS, Philp N, Mears AJ, Swaroop A, Williams DS, Pugh EN Jr. Cone-like morphological, molecular, and electrophysiological features of the photoreceptors of the Nrl knockout mouse. Invest Ophthalmol Vis Sci 2005;46:2156–2167. [PubMed: 15914637]
31. Kobayashi M, Takezawa S, Hara K, Yu RT, Umesono Y, Agata K, Taniwaki M, Yasuda K, Umesono K. Identification of a photoreceptor cell-specific nuclear receptor. Proc Natl Acad Sci USA 1999;96:4814–4819. [PubMed: 10220376]
32. Bumsted O'Brien KM, Cheng H, Jiang Y, Schulte D, Swaroop A, Hendrickson AE. Expression of photoreceptor-specific nuclear receptor NR2E3 in rod photoreceptors of fetal human retina. Invest Ophthalmol Vis Sci 2004;45:2807–2812. [PubMed: 15277507]
33. Cheng H, Khanna H, Oh EC, Hicks D, Mitton KP, Swaroop A. Photoreceptor-specific nuclear receptor NR2E3 functions as a transcriptional activator in rod photoreceptors. Hum Mol Genet 2004;13:1563–1575. [PubMed: 15190009]
34. Chen J, Rattner A, Nathans J. The rod photoreceptor-specific nuclear receptor Nr2e3 represses transcription of multiple cone-specific genes. J Neurosci 2005;25:118–129. [PubMed: 15634773]
35. Peng GH, Ahmad O, Ahmad F, Liu J, Chen S. The photoreceptor-specific nuclear receptor Nr2e3 interacts with Crx and exerts opposing effects on the transcription of rod versus cone genes. Hum Mol Genet 2005;14:747–764. [PubMed: 15689355]
36. Wright AF, Reddick AC, Schwartz SB, Ferguson JS, Aleman TS, Kellner U, Jurklies B, Schuster A, Zrenner E, Wissinger B, et al. Mutation analysis of *NR2E3* and *NRL* genes in enhanced S-cone syndrome. Hum Mutat 2004;24:439. [PubMed: 15459973]
37. Jacobson SG, Sumaroka A, Aleman TS, Cideciyan AV, Schwartz SB, Roman AJ, McInnes RR, Sheffield VC, Stone EM, Swaroop A, et al. Nuclear receptor *NR2E3* gene mutations distort human retinal laminar architecture and cause an unusual degeneration. Hum Mol Genet 2004;13:1893–1902. [PubMed: 15229190]
38. Sharon D, Sandberg MA, Caruso RC, Berson EL, Dryja TP. Shared mutations in NR2E3 in enhanced S-cone syndrome, Goldmann-Favre syndrome, and many cases of clumped pigmentary retinal degeneration. Arch Ophthalmol 2003;121:1316–1323. [PubMed: 12963616]
39. Milam AH, Rose L, Cideciyan AV, Barakat MR, Tang WX, Gupta N, Aleman TS, Wright AF, Stone EM, Sheffield VC, et al. The nuclear receptor NR2E3 plays a role in human retinal photoreceptor differentiation and degeneration. Proc Natl Acad Sci USA 2002;99:473–478. [PubMed: 11773633]
40. Haider NB, Jacobson SG, Cideciyan AV, Swiderski R, Streb LM, Searby C, Beck G, Hockey R, Hanna DB, Gorman S, et al. Mutation of a nuclear receptor gene, *NR2E3*, causes enhanced S cone syndrome, a disorder of retinal cell fate. Nat Genet 2000;24:127–131. [PubMed: 10655056]
41. Marmor MF, Jacobson SG, Foerster MH, Kellner U, Weleber RG. Diagnostic clinical findings of a new syndrome with night blindness, maculopathy, and enhanced S cone sensitivity. Am J Ophthalmol 1990;110:124–134. [PubMed: 2378376]
42. Jacobson SG, Marmor MF, Kemp CM, Knighton RW. SWS (blue) cone hypersensitivity in a newly identified retinal degeneration. Invest Ophthalmol Vis Sci 1990;31:827–838. [PubMed: 2335450]
43. Chen J, Rattner A, Nathans J. Effects of L1 retrotransposon insertion on transcript processing, localization, and accumulation: lessons from the retinal degeneration 7 mouse and implications for the genomic ecology of L1 elements. Hum Mol Genet 2006;15:2146–2156. [PubMed: 16723373]
44. Haider NB, Naggert JK, Nishina PM. Excess cone cell proliferation due to lack of a functional NR2E3 causes retinal dysplasia and degeneration in rd7/rd7 mice. Hum Mol Genet 2001;10:1619–1626. [PubMed: 11487564]
45. Akhmedov NB, Piriev NI, Chang B, Rapoport AL, Hawes NL, Nishina PM, Nusinowitz S, Heckenlively JR, Roderick TH, Kozak CA, et al. A deletion in a photoreceptor-specific nuclear receptor mRNA causes retinal degeneration in the *rd7* mouse. Proc Natl Acad Sci USA 2000;97:5551–5556. [PubMed: 10805811]
46. Corbo JC, Cepko CL. A hybrid photoreceptor expressing both rod and cone genes in a mouse model of enhanced S-cone syndrome. PLoS Genet 2005;1:e11. [PubMed: 16110338]
47. Calvert PD, Krasnoperova NV, Lyubarsky AL, Isayama T, Nicolo M, Kosaras B, Wong G, Gannon KS, Margolskee RF, Sidman RL, et al. Phototransduction in transgenic mice after targeted deletion

of the rod transducin alpha-subunit. Proc Natl Acad Sci USA 2000;97:13913–13918. [PubMed: 11095744]

48. Furukawa T, Morrow EM, Li T, Davis FC, Cepko CL. Retinopathy and attenuated circadian entrainment in Crx-deficient mice. Nat Genet 1999;23:466–470. [PubMed: 10581037]
49. Akimoto M, Filippova E, Gage PJ, Zhu X, Craft CM, Swaroop A. Transgenic mice expressing Cre-recombinase specifically in M- or S-cone photoreceptors. Invest Ophthalmol Vis Sci 2004;45:42–47. [PubMed: 14691152]
50. McKenna NJ, O'Malley BW. Combinatorial control of gene expression by nuclear receptors and coregulators. Cell 2002;108:465–474. [PubMed: 11909518]
51. King-Jones K, Thummel CS. Nuclear receptors–a perspective from Drosophila. Nat Rev Genet 2005;6:311–323. [PubMed: 15803199]
52. Perissi V, Rosenfeld MG. Controlling nuclear receptors: the circular logic of cofactor cycles. Nat Rev Mol Cell Biol 2005;6:542–554. [PubMed: 15957004]
53. Arias AM, Hayward P. Filtering transcriptional noise during development: concepts and mechanisms. Nat Rev Genet 2006;7:34–44. [PubMed: 16369570]
54. Giguere V. Orphan nuclear receptors: from gene to function. Endocr Rev 1999;20:689–725. [PubMed: 10529899]
55. Furukawa A, Koike C, Lippincott P, Cepko CL, Furukawa T. The mouse Crx 5′-upstream transgene sequence directs cell-specific and developmentally regulated expression in retinal photoreceptor cells. J Neurosci 2002;22:1640–1647. [PubMed: 11880494]
56. Zareparsi S, Hero A, Zack DJ, Williams RW, Swaroop A. Seeing the unseen: microarray-based gene expression profiling in vision. Invest Ophthalmol Vis Sci 2004;45:2457–2462. [PubMed: 15277464]
57. Aleman TS, LaVail MM, Montemayor R, Ying G, Maguire MM, Laties AM, Jacobson SG, Cideciyan AV. Augmented rod bipolar cell function in partial receptor loss: an ERG study in P23H rhodopsin transgenic and aging normal rats. Vision Res 2001;41:2779–2797. [PubMed: 11587727]
58. Cideciyan AV, Jacobson SG. An alternative phototransduction model for human rod and cone ERG a-waves: normal parameters and variation with age. Vision Res 1996;36:2609–2621. [PubMed: 8917821]
59. Lyubarsky AL, Falsini B, Pennesi ME, Valentini P, Pugh EN Jr. UV- and midwave-sensitive cone-driven retinal responses of the mouse: a possible phenotype for coexpression of cone photopigments. J Neurosci 1999;19:442–455. [PubMed: 9870972]

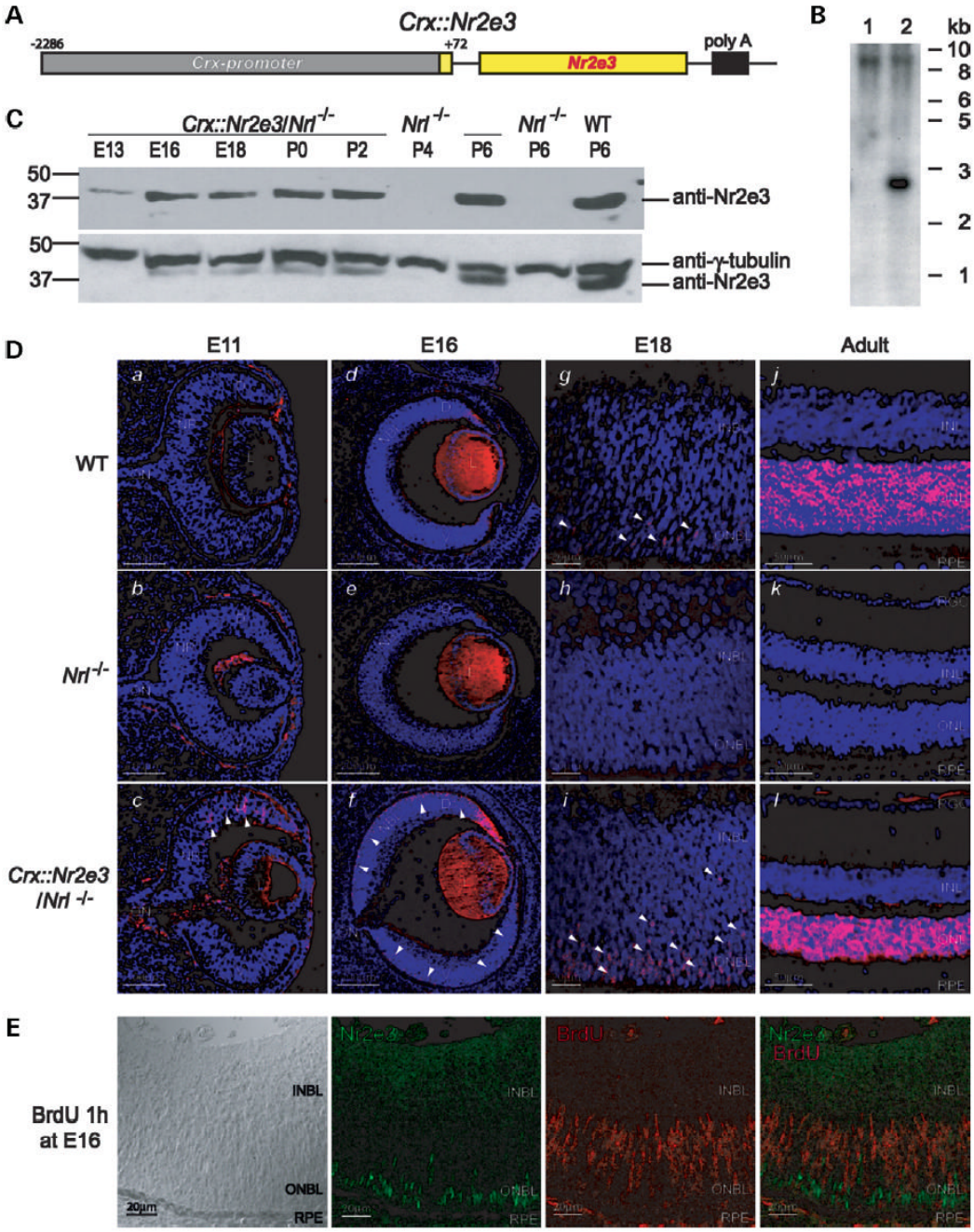

Figure 1.

Temporal and spatial expression of NR2E3 in the *Crx::Nr2e3/Nrl*$^{-/-}$ transgenic mice. (**A**) *Crx::Nr2e3* construct. (**B**) Southern analysis of genomic DNA from *Nrl*$^{-/-}$ (lane 1) and *Crx::Nr2e3/Nrl*$^{-/-}$ (lane 2) mice. The endogenous *Nr2e3* gene is represented by a 9 kb and the transgene by a 2.8 kb band. (**C**) Immunoblot analysis of neural retina extract shows the temporal expression of NR2E3 in the *Crx::Nr2e3/Nrl*$^{-/-}$ mice during the early developmental stages, compared with *Nrl*$^{-/-}$ and WT mice. γ-tubulin is used as an internal control. (**D**) Immunostaining with anti-NR2E3 antibody (red, indicated as arrowhead) showing spatial expression of NR2E3 in the *Crx::Nr2e3/Nrl*$^{-/-}$ mice, compared with WT and *Nrl*$^{-/-}$ mice, at E11, E16, E18 and 4 week. In the WT retina, *NR2E3* is expressed only in the rods and not

cones (32–35). In the *Crx::Nr2e3/Nrl*$^{-/-}$ retina, *NR2E3* is expressed in both rods and cones because of the *Crx* promoter that is used. The staining in the WT retina appears somewhat patchy because of the short exposure time to avoid saturating the signal in most of the cells and a somewhat uneven retinal section. (**E**) Immunostaining with anti-NR2E3 and BrdU antibodies after 1 h pulse of BrdU injection at E16. No colocalization is observed in the retinal section. ON, optic nerve; NR, neural retina; D, dorsal; L, lens; V, ventral; NBL, neuroblastic layer; ONBL, outer neuroblastic layer; INBL, inner neuroblastic layer; RPE, retinal pigment epithelium; RGC, retinal ganglion cells. Scale bars are indicated.

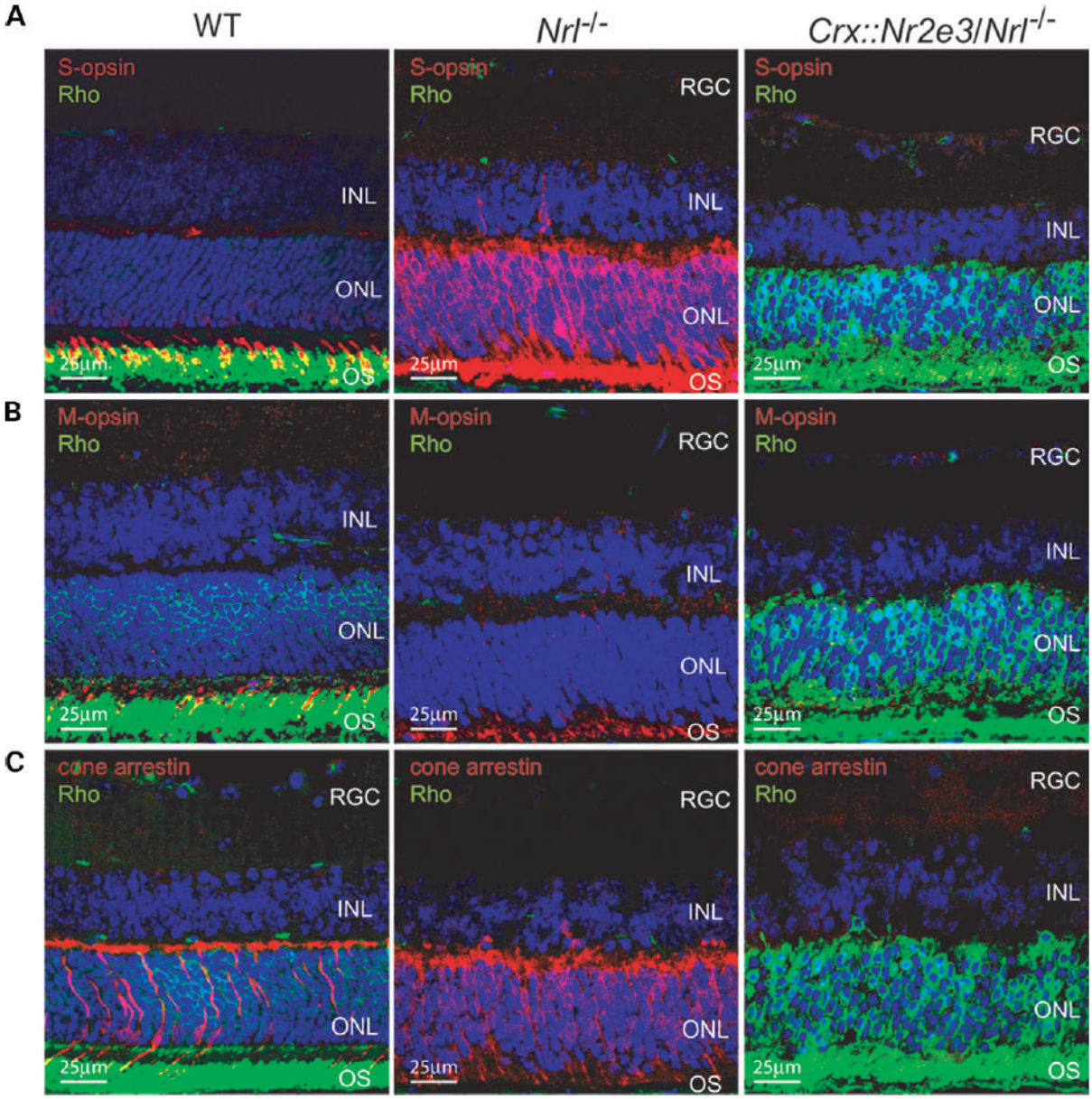

Figure 2.

IHC of photoreceptor markers in the WT, *Nrl*$^{-/-}$ and *Crx::Nr2e3/Nrl*$^{-/-}$ mice. (**A**–**C**) Immunostaining with anti-S-opsin (A), M-opsin (B), cone arrestin (C) and rhodopsin antibodies. Rhodopsin is detected in the ONL and OS of the WT and *Crx::Nr2e3/Nrl*$^{-/-}$ retina. S-opsin and cone arrestin are enriched in the *Nrl*$^{-/-}$ retina but are undetectable in the *Crx::Nr2e3/Nrl*$^{-/-}$ retina. M-opsin is undetectable in the transgenic mice. RPE, retinal pigment epithelium; RGC, retinal ganglion cells. Scale bars are indicated.

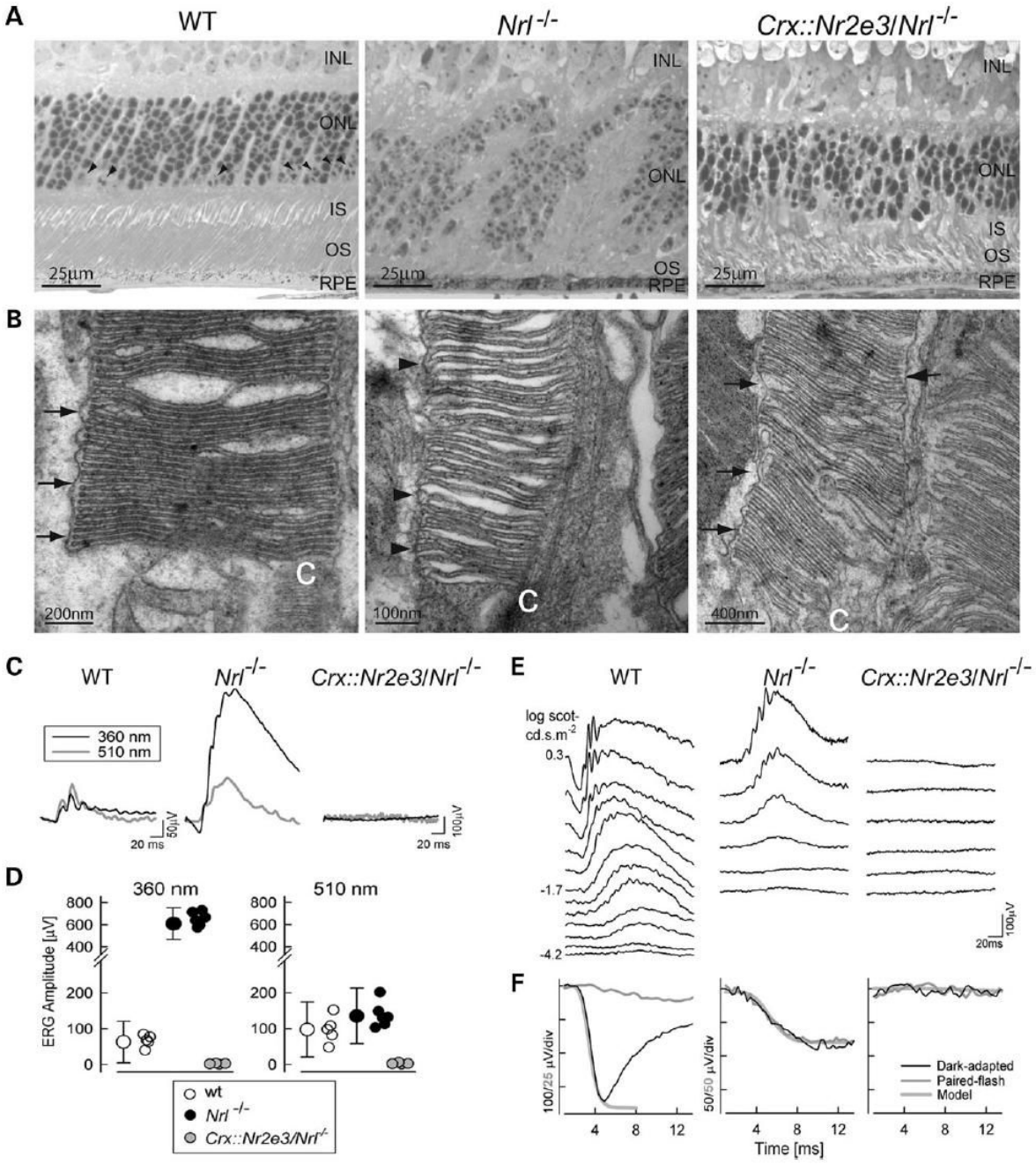

Figure 3.

Rescue of rod morphology but not function in the *Crx::Nr2e3/Nrl*$^{-/-}$ mice by NR2E3. (**A**) Toluidine blue staining of the retina section demonstrates that the nuclei of photoreceptors in the *Crx::Nr2e3/Nrl*$^{-/-}$ retina exhibit a rod-like morphology, unlike the cones observed in the *Nrl*$^{-/-}$ retina. Arrows in the WT section refer to staining of cone nuclei. (**B**) TEM shows closed discs with distorted orientation in the photoreceptor outer segments of the *Crx::Nr2e3/Nrl*$^{-/-}$ retina, compared with WT and *Nrl*$^{-/-}$ mice. Arrows indicate OS membrane surrounding the discs, whereas arrowheads indicate the open discs of cones. (**C**) Light-adapted, spectral ERGs that evoke nearly matched responses from S-cones (360 nm, black traces) or M-cones (510 nm, gray traces) in WT are not detect-$^{-/-}$ mouse and are largely mismatched in *Nrl*$^{-/-}$. (**D**)

Spectral ERG amplitudes demonstrate the enrichment of S-cone activity (360 nm) able in a *Crx::Nr2e3/Nrl*$^{-/-}$ mice compared with WT. *Crx::Nr2e3/Nrl*$^{-/-}$ in *Nrl*$^{-/-}$ mice (gray symbols) show responses indistinguishable from noise. (**E**) Dark-adapted ERGs evoked by increasing intensities of blue flashes in *Nrl*$^{-/-}$ mice show elevated thresholds (by ~3 log units) compared with WT. The *Crx::Nr2e3/Nrl*$^{-/-}$ mouse shows no detectable ERGs. (**F**) Leading edges of dark-adapted ERG photoresponses evoked by a pair of white flashes (3.6 log scot-cd.s.m^{-2}) presented 4 s apart and fit with a model of phototransduction activation (smooth grey lines). In WT mice, rods dominate the first flash photoresponse (dark line); the paired-flash has a smaller, cone-mediated response (grey line). In *Nrl*$^{-/-}$ mice, dark-adapted photoresponses are smaller and slower than WT; the paired-flash response closely tracks the first flash response. ERG photoresponses are not detectable in the *Crx::Nr2e3/Nrl*$^{-/-}$ mice. RPE, retinal pigment epithelium; IS, photoreceptor inner segment. Scale bars are indicated.

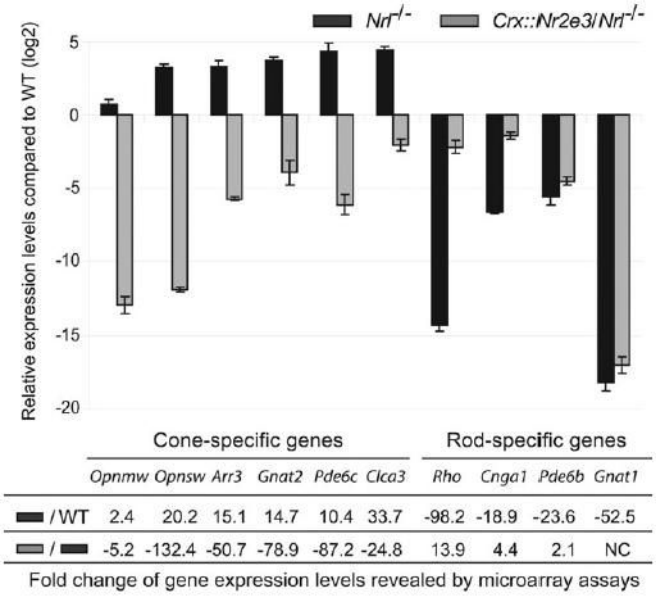

Figure 4.

qPCR analysis of the selected phototransduction genes. qPCR analysis using WT, *Nrl*$^{-/-}$ and *Crx::Nr2e3/Nrl*$^{-/-}$ retinal RNA shows that the expression of cone-specific genes is suppressed while those of rod genes, except *Gnat1*, restored to varying degree. Expression levels are normalized to the housekeeping gene *Hprt* first and then compared with WT. Error bars show the standard deviation. The actual fold change of gene expression levels revealed by microarray assays is shown in the table below. NC, no change. Gene symbols are: M-opsin or green cone opsin (*Opn1mw*), S-opsin or blue cone opsin (*Opn1sw*), cone arrestin (*Arr3*), cone transducin (*Gnat2*), phosphodiesterase 6c (*Pde6c*), chloride channel calcium-activated 3 (*Clca3*), rhodopsin (*Rho*), cyclic nucleotide-gated channel α-1 (*Cnga1*), phosphodiesterase β subunit (*Pde6b*) and rod transducin (*Gnat1*).

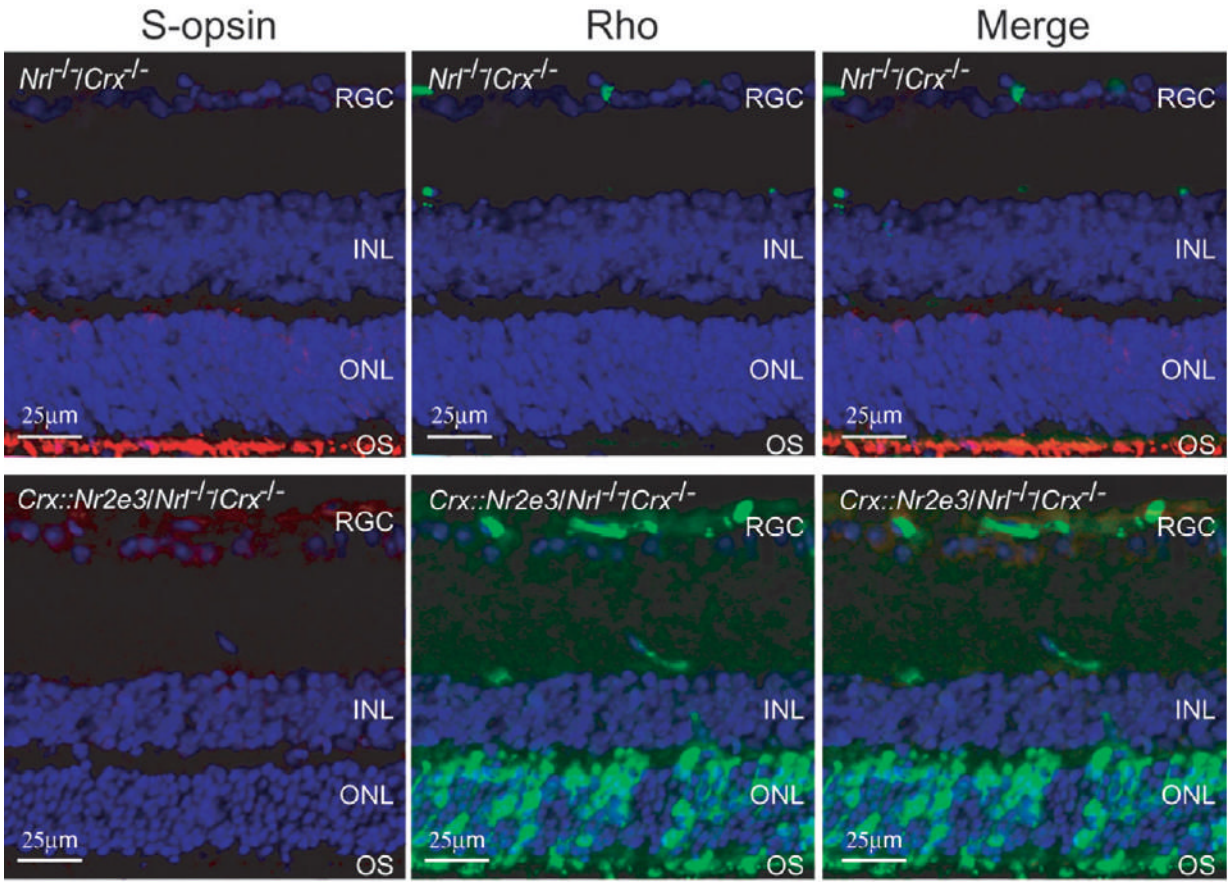

Figure 5.

IHC of photoreceptor markers in the *Nrl*$^{-/-}$/*Crx*$^{-/-}$ and *Crx::Nr2e3/Nrl*$^{-/-}$/*Crx*$^{-/-}$ mice. Immunostaining with anti-S-opsin and rhodopsin anti-bodies, showing that S-opsin is increased and rhodopsin is absent in the *Nrl*$^{-/-}$/*Crx*$^{-/-}$ retina. However, in the *Crx::Nr2e3/Nrl*$^{-/-}$/*Crx*$^{-/-}$ retina, S-opsin is absent and rhodopsin is expressed. RPE, retinal pigment epithelium; RGC, retinal ganglion cells. Scale bars are indicated.

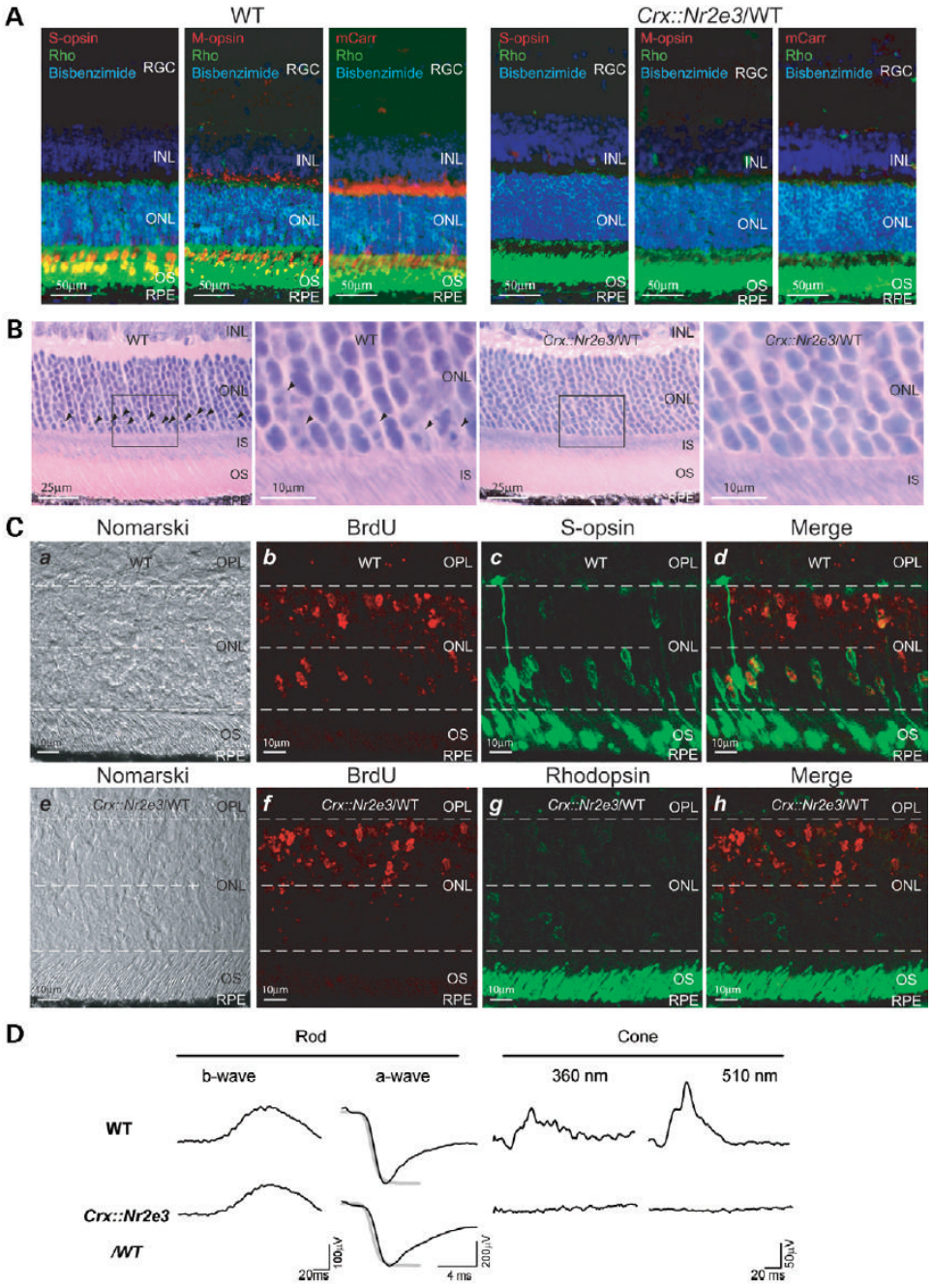

Figure 6.

Crx::Nr2e3 transgene in the WT background. (**A**) Immunostaining with anti S-opsin, M-opsin, cone arrestin and rhodopsin antibodies of WT, and *Crx::NR2e3/*WT retina shows that cone markers are undetectable in the transgenic mice. (**B**) Toluidine blue staining of the WT and *Crx::Nr2e3/*WT retina demonstrates the cone-like nuclear staining (indicated by arrows) in the WT retina but not in the transgenic mice. The image in black rectangle shows higher magnification. (**C**) Anti-BrdU labeling of 3 week retina after a single injection of BrdU at E14. The amount of strongly BrdU-labeled cells in the ONL is not significantly different between WT and transgenic groups. In WT mice, these cells are located to either outer or inner part of ONL, with cells in the outermost regions co-localizing with S-opsin. However, in the transgenic

retina, most of these cells are present in the inner part of ONL. Dashed lines demonstrate the inner and outer half of the ONL. (**D**) *Crx::Nr2e3/*WT mice show normal rod function but undetectable cone function. Rod ERGs elicited by a dim (b-wave) and bright flash (a-wave) in the dark show similar responses in *Crx::Nr2e3*/WT and WT mice. A model (smooth gray lines) fit to the responses show normal phototransduction activation. Light-adapted, cone-mediated spectral ERGs (evoked as in Fig. 2C) are not detectable in the *Crx::Nr2e3*/WT mouse. RPE, retinal pigment epithelium; IS, photoreceptor inner segment; RGC, retinal ganglion cells. Scale bars as indicated.

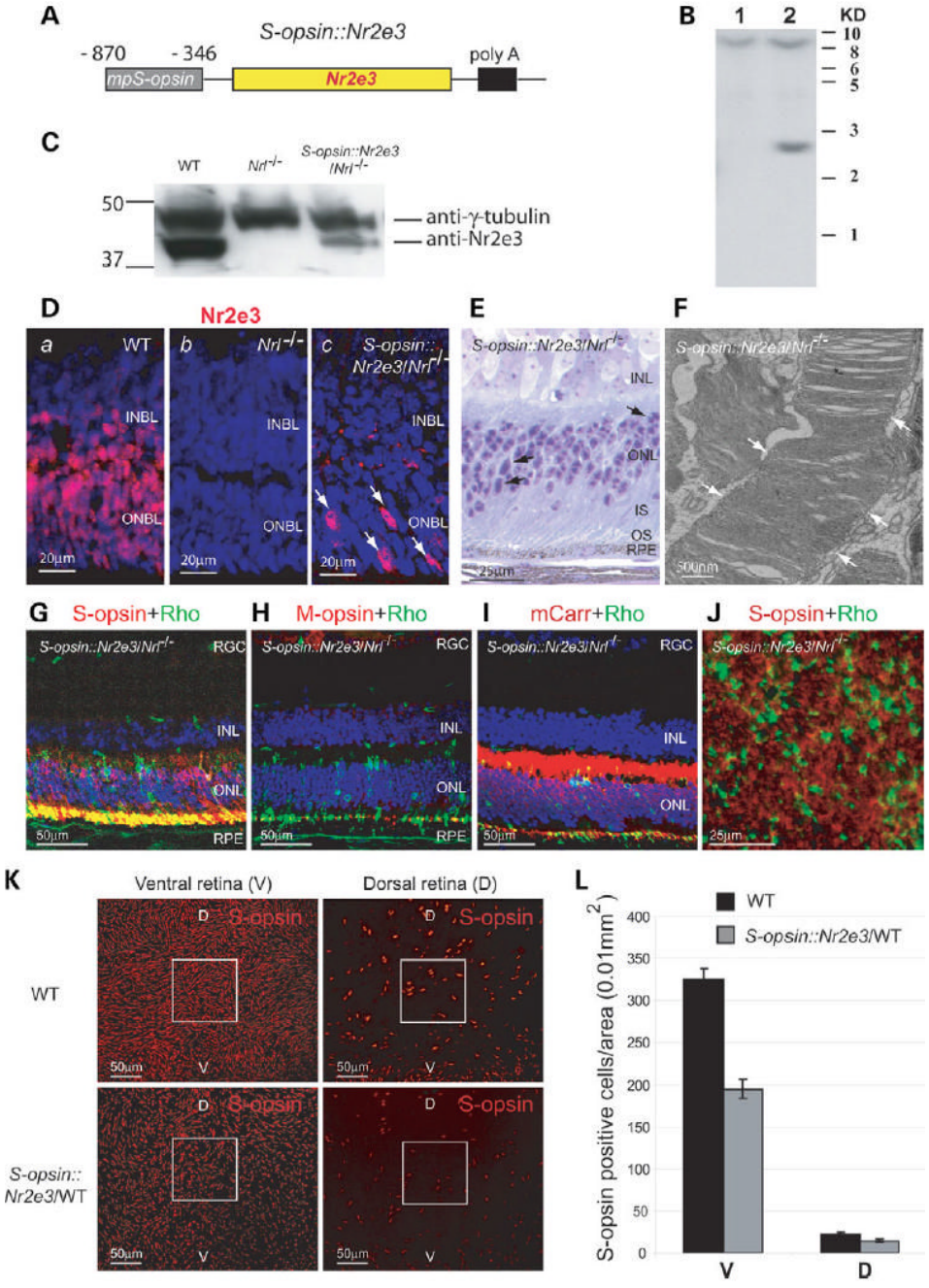

Figure 7.

Dual function of ectopically expressed *Nr2e3* in the *S-opsin::Nr2e3* transgenic mice. (**A**) *S-opsin::Nr2e3* construct. (**B**) Southern blotting of genomic DNA from $Nrl^{-/-}$ (lane 1) and *S-opsin::Nr2e3/*$Nrl^{-/-}$ (lane 2) mice. The endogenous *Nr2e3* gene is represented by a 9 kb and the transgene by a 2.8 kb band. (**C**) Immunoblot analysis of neural retina extract shows the expression of NR2E3 protein in the *S-opsin::Nr2e3/*$Nrl^{-/-}$ mice at P6, compared with the $Nrl^{-/-}$ and WT mice. γ-tubulin is used as an internal control. (**D**) Immunostaining with anti-NR2E3 antibody (red, indicated as arrows) showing signal of NR2E3 staining in *S-opsin::Nr2e3/*$Nrl^{-/-}$ mice (*c*), compared with WT (*a*) and $Nrl^{-/-}$ mice (*b*), at P6. (**E**) Toluidine blue staining of the retina section demonstrates that several nuclei of photoreceptors in *S-*

opsin::Nr2e3/Nrl$^{-/-}$ mouse change from cone-like to rod-like morphology. Photoreceptors in the *Nrl*$^{-/-}$ retina exhibit cone morphology (see Fig. 2A). Rod-like nuclei are indicated by arrows. (**F**) TEM shows closed discs with distorted orientation in the photoreceptor outer segment of the *S-opsin::Nr2e3/Nrl*$^{-/-}$ mouse, compared with WT and *Nrl* $^{-/-}$ mice (see Fig. 2B). Arrows indicate OS membrane surrounding the discs. (**G**–**J**) Immunostaining with anti-S-opsin (G, J), M-opsin (H), cone arrestin (I) and rhodopsin antibodies. Rhodopsin is detected in the ONL and OS of the *S-opsin::Nr2e3/Nrl*$^{-/-}$ retina. No obvious co-localization of S-opsin and rhodopsin is observed in the retinal flat mount (J). (**K**) Immunostaining with cone photoreceptor marker (S-opsin) antibody in the WT and *S-opsin::Nr2e3/*WT flat mount retina. Dorsal–ventral pattern of S-opsin gradient is still preserved in the transgenic mice. Reduced numbers of S-opsin positive cells are observed in the *S-opsin::Nr2e3/*WT retina. (**L**) Cell counting of S-opsin positive cells on the WT and *S-opsin/*WT flat mount retina stained with anti S-opsin antibody. S-opsin positive cells were counted in two regions: in the middle of ventral retina (V), and in the middle of dorsal retina (D). A square of 100 μm × 100 μm area, indicated in (K) was used to count the S-opsin positive cells and three mice were tested. ONBL, outer neuroblastic layer; INBL, inner neuroblastic layer; RPE, retinal pigment epithelium; IS, inner segments; RGC, retinal ganglion cells; V, ventral; D, dorsal. Scale bars as indicated.

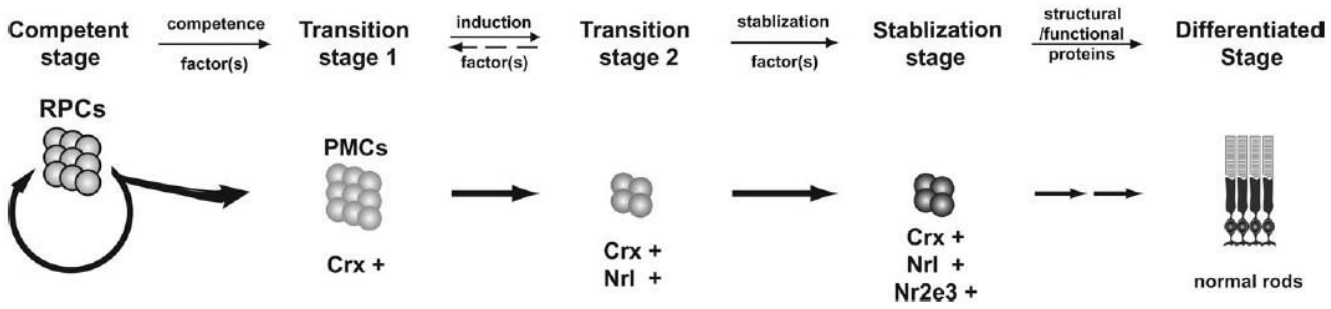

Figure 8.

A schematic representation of NR2E3 function during photoreceptor development. RPCs undergo terminal mitosis at specific times during development. The post-mitotic cells (PMCs) expressing CRX are directed towards photoreceptor lineage and pass through distinct transition stages. PMCs that actively express NRL are instructed to rod cell fate, whereas those without NRL produce cones. Ectopic expression of NR2E3 in the latter will repress cone genes and produce rod-like characteristics. The expression of NRL induces rod differentiation, but only subsequent NR2E3 expression stabilizes the cell fate by repressing cone genes.

Table 1

Non-redundant differentially expressed genes common in two gene profile comparisons

Gene symbol	Gene title	AFC-*Nrl*$^{-/-}$ versus WT 4 week	AFC-Nr2e3 transgenic versus *Nrl*$^{-/-}$ 4 week	GO biological process description
Casp7	Caspase 7	7.83	−60.85	Proteolysis/apoptosis
Ampd2	Adenosine monophosphate deaminase 2(isoform L)	14.24	−58.80	Nucleotide metabolism
Pde6h	Phosphodiesterase 6H, cGMP-specific, cone, gamma	9.70	−52.12	Activation of MAPK activity/visual perception
Kcne2	Potassium voltage-gated channel, Isk-related subfamily, gene 2	9.89	−47.75	Potassium ion transport
Aplp1	Amyloid beta (A4) precursor-like protein 1	8.14	−40.39	Endocytosis/apoptosis/forebrain development
Cxx1c	CAAX box 1 homolog C (human)	19.31	−25.50	
Crot	Carnitine-*O*-octanoyltransferase	23.17	−24.25	Fatty acid transport
Fkbp9	FK506 binding protein 9	24.10	−21.70	Protein folding
Elovl5	ELOVL family member 5, elongation of long-chain fatty acids (yeast)	13.30	−19.35	Metabolism
Fabp7	Fatty acid-binding protein 7, brain	30.59	−18.62	Transport
4930544G21Rik	RIKEN 4930544G21 gene	5.54	−18.01	
7530404M11Rik	RIKEN 7530404M11 gene	14.65	−16.66	
Wwp1	WW domain containing E3 ubiquitin protein ligase 1	8.47	−16.37	Ubiquitin cycle/negative regulation of transcription
Igsf4b	Immunoglobulin superfamily, member 4B	8.87	−16.17	Protein localization/cell adhesion
Prickle2	Prickle-like 2 (*Drosophila*)	7.78	−15.50	
Apeg1	Aortic preferentially expressed gene 1	7.70	−15.24	Protein amino acid phosphorylation
Kcnd3	Potassium voltage-gated channel, Shal-related family, member 3	3.95	−14.83	Potassium ion transport
Cngb3	Cyclic nucleotide gated channel beta 3	22.41	−12.25	Potassium ion transport/visual perception
Nrxn3	Neurexin III	3.07	−11.61	Synaptogenesis
BC037006	cDNA BC037006	14.32	−10.75	
Klhl4	Kelch-like 4 (*Drosophila*)	7.39	−10.07	
C030009J22Rik	RIKEN C030009J22 gene	7.33	−10.01	
4930458D05Rik	RIKEN cDNA 4930458D05 gene	14.34	−9.92	Metabolism
Clic4	Chloride intracellular channel 4 (mitochondrial)	6.69	−8.98	Cell differentiation/chloride transport
C130076O07Rik	RIKEN C130076O07 gene	11.06	−8.96	Cell adhesion/neuron migration/ synaptogenesis
LOC553091	Hypothetical LOC553091	4.17	−8.82	
Cckbr	Cholecystokinin B receptor	11.72	−8.39	G-protein coupled receptor protein signaling pathway
Usp46	Ubiquitin specific peptidase 46	7.75	−8.23	Ubiquitin-dependent protein catabolism
Bmp15	Bone morphogenetic protein 15	2.98	−8.10	Signaling pathway
Klf3	Kruppel-like factor 3 (basic)	12.02	−7.78	Regulation of transcription
4921511K06Rik	RIKEN cDNA 4921511K06 gene	6.16	−7.51	
Tcta	T-cell leukemia translocation altered gene	3.89	−7.20	
Igsf3	Immunoglobulin superfamily, member 3	5.32	−6.84	
Guca1a	Guanylate cyclase activator 1a (retina)	NC	−6.78	Visual perception/phototransduction
Arhgdib	Rho, GDP dissociation inhibitor (GDI) beta	6.30	−6.74	
Notch2	Notch gene homolog 2 (Drosophila)	5.78	−6.68	Regulation of transcription/signaling pathway
Ptprg	Protein tyrosine phosphatase, receptor, G	5.02	−6.60	Protein tyrosine phosphatase signaling pathway
Gabrb3	Gamma-aminobutyric acid (GABA-A) receptor, subunit beta 3	3.38	−6.54	Chloride transport/gamma-aminobutyric acid signaling pathway
Pank1	Pantothenate kinase 1	4.56	−6.22	Coenzyme A biosynthesis
Ube2e1	Ubiquitin-conjugating enzyme E2E 1, UBC4/5 homolog (yeast)	3.21	−6.11	Ubiquitin-dependent protein catabolism/ ubiquitin cycle
Mtap6	Microtubule-associated protein 6	6.59	−6.07	Microtubule-based process
Olfm1	Olfactomedin 1	8.12	−6.00	Development
Dirc2	Disrupted in renal carcinoma 2	8.52	−5.91	
Smug1	Single-strand selective monofunctional uracil DNA glycosylase	NC	−5.87	Carbohydrate metabolism/DNA repair

Hum Mol Genet. Author manuscript; available in PMC 2006 October 10.

Gene symbol	Gene title	AFC-*Nrl*$^{-/-}$ versus WT 4 week	AFC-Nr2e3 transgenic versus *Nrl*$^{-/-}$ 4 week	GO biological process description
Calu	Calumenin	4.84	−5.85	
Pygm	Muscle glycogen phosphorylase	4.78	−5.74	Glycogen metabolism
Tmsb10	Thymosin, beta 10	4.88	−5.62	Actin cytoskeleton organization
4933413A10Rik	RIKEN 4933413A10 gene	5.85	−5.62	
Tuft1	Tuftelin 1	4.04	−5.48	Bone mineralization/odontogenesis
Ece1	Endothelin converting enzyme 1	6.09	−5.45	Proteolysis
Gem	GTP-binding protein (over-expressed in muscle)	6.23	−5.38	Small GTPase mediated signal transduction
Smpdl3a	Sphingomyelin phosphodiesterase, acid-like 3A	6.41	−5.35	Carbohydrate metabolism
Pcdha4	Protocadherin alpha	6.97	−5.24	Cell adhesion
Arid5b	Modulator recognition factor 2 (Mrf2)	3.42	−5.16	Regulation of transcription
Acsl3	Acyl-CoA synthetase long-chain family member 3	2.61	−5.09	Fatty acid metabolism
E130012K09	Hypothetical protein E130012K09	5.65	−5.07	
Elovl2	Elongation of very long chain fatty acids (FEN1/Elo2)-like 2	2.98	−5.07	Very-long-chain fatty acid metabolism
Hbb	Hemoglobin, beta adult minor chain	NC	−5.06	Oxygen transport
4631427C17Rik	RIKEN 4631427C17 gene	3.82	−5.05	Metabolism
Cuedc1	CUE domain containing 1	3.08	−5.00	
Acbd6	Acyl-Coenzyme A binding domain containing 6	4.49	−4.97	
A430031N04	Hypothetical protein A430031N04	4.37	−4.93	
Scg3	Secretogranin III	7.25	−4.83	
Pard6b	Par-6 (partitioning defective 6) homolog beta	2.54	−4.81	Cell cycle/intracellular signaling cascade
Calm1	Calmodulin 1	2.35	−4.78	Cell cycle/G-protein coupled receptor protein signaling pathway
Gas2	Growth arrest specific 2	2.36	−4.75	Apoptosis/cell cycle
Eya1	Eyes absent 1 homolog (Drosophila)	7.04	−4.68	Regulation of transcription/apoptosis
Pdha1	Pyruvate dehydrogenase E1 alpha 1	NC	−4.68	Glycolysis/metabolism
Pnp	purine-nucleoside phosphorylase	8.09	−4.64	Nucleic acid metabolism
Plec1	Plectin 1	4.17	−4.63	Protein ADP-ribosylation
Ppapdc1	Phosphatidic acid phosphatase type 2 domain containing 1	3.22	−4.62	
Galnt13	UDP-*N*-acetyl-alpha-D-galactosamine:polypeptide *N*-acetylgalactosaminyl-transferase 13	8.42	−4.54	Protein amino acid O-linked glycosylation
Ddhd2	DDHD domain 2	4.00	−4.51	
6620401M08Rik	RIKEN 6620401M08 gene	3.56	−4.49	
Elovl6	ELOVL family member 6, elongation of long chain fatty acids (yeast)	7.16	−4.37	Fatty acid elongation/metabolism
1110002B05Rik	RIKEN 1110002B05 gene	3.43	−4.34	
St3gal3	ST3 beta-galactoside alpha-2,3-sialyltransferase 3	7.69	−4.31	Protein amino acid glycosylation
Mpp6	MAGUK p55 subfamily member 6	7.76	−4.27	
Rpl5	Ribosomal protein L5	2.11	−4.24	Protein biosynthesis
Moxd1	Monooxygenase, DBH-like 1	5.04	−4.15	Catecholamine metabolism
Crxos1	Crx opposite strand transcript 1	5.38	−4.10	Regulation of transcription
St8sia1	ST8 alpha-*N*-acetyl-neuraminide alpha-2, 8-sialyltransferase 1	−10.75	3.81	Protein amino acid glycosylation/cell proliferation
Lrrc2	Leucine-rich repeat containing 2	−4.05	7.58	
Kcnj14	Potassium inwardly-rectifying channel, subfamily J, member 14	−25.28	7.91	Potassium ion transport
Slc24a1	Solute carrier family 24 (sodium/potassium/calcium exchanger), member 1	−34.78	12.12	Calcium ion transport/visual perception

(i) Nrl-knockout (*Nrl::GFP/Nrl*$^{-/-}$) versus WT (*Nrl::GFP*/WT) retina (21); and (ii) NR2E3-expressing (*Nrl::GFP/Crx::Nr2e3/Nrl*$^{-/-}$) transgenic versus Nrl-knockout (*Nrl::GFP/Nrl*$^{-/-}$) retina. FACS-sorted GFP + cells from 4-week-old mouse retina were used for gene profiling. Only genes with a minimum fold change of 4 and FDRCI *P*-value of <0.1 from comparison (ii) are selected. AFC, average fold change; NC, no change.